Computer graphics presentations and analysis of hydrogen bonds from molecular dynamics simulation

Masayuki Shibata

Department of Biophysics, Roswell Park Cancer Institute, Buffalo, NY, USA

Theresa Julia Zielinski

Department of Chemistry, Niagara University, Niagara University, NY, USA

To obtain better insights into the dynamic nature of hydrogen bonding, computer graphics representations were introduced as an aid for the analysis of molecular dynamics trajectories. A schematic representation of hydrogen bonding patterns is generated to reflect the frequency and the type of hydrogen bonding occurring during the simulation period. Various trajectory plots for monitoring geometrical parameters and for analyzing three-center hydrogen bonding were also generated. The methods proposed are applicable to a variety of biopolymers. In this study, hydrogen bonding in the $d(G)_6 \cdot d(C)_6$ system was examined. For the nucleic acid fragments examined, three-center hydrogen bonds can be classified as in-plane and major or minor groove types. The in-plane three-center hydrogen bond represents a stable state in which both bonds simultaneously satisfy the relaxed hydrogen bonding criteria for a measurable period. On the other hand, groove three-center hydrogen bonds behave as a transient intermediate state in a flip-flop hydrogen bonding system.

Keywords: three-center hydrogen bond, unusual hydrogen bond, flip-flop hydrogen bond, molecular dynamics simulation, base pair, Watson-Crick hydrogen bond

INTRODUCTION

Hydrogen bonding is one of the most important molecular phenomena. It plays a vital role in the structure and function of various interesting molecules, e.g., it is responsible for the secondary and tertiary structural features of proteins and nucleic acids. In aqueous solution the hydrogen bonding property of water molecules also plays an essential role in the structure and function of biological macromolecules. Thus it is not surprising that there are numerous books and review articles on the hydrogen bonding of small molecules and biomacromolecules, ranging from gaseous to the solution or solid states.[1–8]

Analysis of hydrogen bonding as it occurs in molecular dynamics (MD) simulations has appeared in the literature. Koehler et al. analyzed the occurrence of three-center hydrogen bonding in cyclodextrins;[9,10] Swanson et al. used the animation technique in their study of hydrogen bonding at the active center of elastin;[11] Nordlund et al. examined the effect of a modified base on the hydrogen bonding of DNA dodecamers;[12] and Fraternali studied the dynamics of hydrogen bonding pattern for the linear peptide ahmethicin.[13]

The MD simulation technique is a useful tool for studying the energetics and structures of biological macromolecules.[14–17] Care must be used when analyzing an MD trajectory because it consists of numerous configurations generated during a simulation period typically ranging from tens to hundreds of picoseconds. For example, if one dihedral angle exists in a (+) gauche conformation for 50% of the time and in a (−) gauche conformation for the rest of the time, simple averaging for the entire simulation period leads to an unrealistic cis (or trans) conformation. Thus it is important to carefully examine the MD trajectories for any property of interest, including hydrogen bonding.

In this article, we propose some computer graphics representations as aids to the analysis of hydrogen bonding occurring during an MD simulation. Schematic representations of hydrogen bonding are generated that reflect the frequency of occurrence during a simulation period. The graphics presentations of hydrogen bonding from an MD trajectory provide more insight into the nature of the hydrogen bond than could be obtained from simple numerical tables. Although the methods proposed are applicable to biopolymers, such as proteins, nucleic acids and carbohydrates, the $d(G)_6 \cdot d(C)_6$ system was taken as an example.

Color Plates for this article are on pages 107–109.

Address reprint requests to Dr. Shibata at the Dept. of Biophysics, Roswell Park Cancer Institute, Elm and Cralton Streets, Buffalo, NY 14263, USA.
Received 25 June 1991; accepted 11 September 1991

The utility of computer graphics presentations in the analysis of three-center hydrogen bonds is also discussed.

METHOD

Since the details of the MD simulation of the DNA hexamer $d(G)_6 \cdot d(C)_6$ were already described elsewhere,[18] only a brief summary is given here. The standard *B*-DNA form[19] was used as an initial geometry and the counterions were positioned at the phosphate groups. The solvent effect was included by modeling the first hydration shell with 292 SPC waters[20] (those within 0.5 nm of any solute atom). The central hydrogen bond of the top and bottom base pairs was restrained to its initial length to prevent fraying of the ends of the helix. Dynamics was initiated with velocities from a 300 K Maxwellian distribution after the initial structure was relaxed by molecular mechanics. The program GROMOS[21] was used without modification. The 60-ps MD simulation was performed by using a step size of 0.001 ps for the first 20 ps and 0.002 ps for the next 40 ps. The trajectories were generated by saving coordinates at every 0.05 ps. Only the final 40 ps were used for analysis.

Hydrogen bonding within the solute molecule was analyzed first with the program PROHB.[21] The donor (D)-to-acceptor (A) distance and the angle D − H · · A are typical geometrical parameters used to define the normal linear (two-center) hydrogen bonds in crystallographic studies in which the position of hydrogens are not easily obtained.[22] Since hydrogen positions are monitored easily in MD studies, the hydrogen (H)–acceptor (A) distance is used as one of hydrogen bonding criteria instead of the D · · A distance. To account for the occurrence of three-center bonds, more relaxed criteria, 0.27 nm for the H · · A distance and 90° for the D–H · · A angle, are used instead of the normal criteria of 0.25 nm and 135°. To observe changes in hydrogen bonding patterns over time during the simulation, the final 40 ps of the trajectory was divided into four 10-ps time spans *T*(21–30), *T*(31–40), *T*(41–50), and *T*(51–60). Some of the results from PROHB are shown in Table 1. This table illustrates some of the difficulties encountered when using numerical tables to study overall hydrogen bonding features, such as the type of hydrogen bond, changes in strength over time, and the identity of donor and acceptor atoms. To overcome this, we developed the strategy of presenting a schematic diagram for hydrogen bonding by using arrows pointing from donor to acceptor. The arrow thickness computed from the frequency of occurrence of the hydrogen bond is used to indicate its strength. The program to generate this presentation is written in standard FORTRAN 77, and the resulting diagram is stored in an HPGL form that can be disposed to HP compatible printers or plotters or can be incorporated into standard word processing or presentation graphics PC programs.

Although Color Plate 1 is more informative than tabular data, the dynamic nature of hydrogen bonding can be appreciated better by monitoring specific geometrical parameters as a function of time. It is even better to monitor two parameters simultaneously. This is accomplished by plotting them in the same diagram. If distance H · · A and angle D–H · · A are chosen, then the left vertical axis can be used for one and the right vertical axis can be used for the other. The distance side can be set to the user specified values, e.g., from 0.15 to 0.35 nm. Each parameter will have its own hydrogen bonding cutoff; the lower limit for the D–H · · A angle and the upper limit for the H · · A distance are drawn as horizontal lines. A scale factor is chosen to make the upper limit for the H · · A distance fall at the same position as the physical maximum limit of the D–H · · A angle (180°). These conditions will automatically set the minimum vertical axis value for the D–H · · A angle and the H · · A distance value corresponding to the lower limit value of 135° (or 90°) for the D–H · · A angle. When the two parameters at any given time remain within the zone enclosed by the upper and lower limit lines, the bond examined satisfies the hydrogen bonding condition. Using a different color for each parameter facilitates differentiating the two behaviors. The results obtained for various types of hydrogen bonds are shown in Color Plates 2a–i.

The large number of hydrogen bond donors and acceptors in nucleic acid bases makes various three-center hydrogen bonding situations feasible. In this case, the two constituent hydrogen bonds are monitored simultaneously. The two H · · A distances and the two D–H · · A angles are plotted against time using different colors to distinguish the major and minor component hydrogen bonds. Since three-center hydrogen bond atoms should be relatively coplanar, the sum

Table 1. Sample hydrogen bonding analysis output

				Atom name			Atom type			Atom number			Geometrical parameters			
Donor		Acceptor		D-	H-	A	D-	H-	A	D-	H-	A	D - H (nm)	H - A (nm)	Angle (°)	D - A (nm)
1	4DGUA -	1	9DCYT	N2-	H21-	O2	NT-	H-	O	86-	87-	201	0.101	0.211	145.6	0.298
1	4DGUA -	1	10DCYT	N2-	H21-	O2	NT-	H-	O	86-	87-	222	0.101	0.230	118.5	0.291
1	4DGUA -	1	9DCYT	N1-	H1-	N3	NR6*-	H-	NR6	89-	90-	202	0.100	0.211	149.4	0.300
1	4DGUA -	1	9DCYT	N1-	H1-	O2	NR6*-	H-	O	89-	90-	201	0.100	0.216	141.7	0.299
1	5DGUA -	1	8DCYT	N2-	H21-	O2	NT-	H-	O	111-	112-	180	0.100	0.204	150.4	0.295
1	5DGUA -	1	9DCYT	N2-	H22-	O2	NT-	H-	O	111-	113-	201	0.101	0.238	115.0	0.293
1	5DGUA -	1	8DCYT	N1-	H1-	N3	NR6*-	H-	NR6	114-	115-	181	0.100	0.206	151.6	0.297
1	5DGUA -	1	8DCYT	N1-	H1-	O2	NR6*-	H-	O	114-	115-	180	0.100	0.221	139.0	0.303
1	5DGUA -	1	4DGUA	N1-	H1-	O6	NR6*-	H-	O	114-	115-	92	0.102	0.241	137.4	0.323

of the angles D–H · · A1, D–H · · A2 and A1 · · H · · A2, and the dihedral angle A1–D–H–A2 must be also examined. A scaling technique similar to that in Color Plates 2a–i is used to draw these two different angles in the same diagram, as shown in Color Plates 3a–l. Although the various plots are useful for analyzing different factors affecting the formation and breakage of three-center bonds, they do not easily portray the frequency and duration of three-center bonds. To overcome this problem, numerical values are assigned to the four possible situations for the two hydrogen bonds potentially involved in a three-center hydrogen bond. For the configuration where all the conditions defining a three-center bond are satisfied (H · · An < 0.27 nm, D–H · · An > 90°, a sum of three angles >340°, and |A1–D–H–A2| < 15°), the value 1.5 is assigned. If the three-center hydrogen bond criteria are not satisfied, then each hydrogen bond is examined separately using the normal linear hydrogen bonding criteria (H · · A < 0.25 nm, D–H–A > 135°). A value of 1 is assigned when D–H · · A1 satisifies the condition, or a value of 2 is assigned when D–H · · A2 satisfies the condition. Finally, if there is no hydrogen bond, the value 0 is assigned. These values are then plotted against time in Figures 1a–c. Simplified diagrams (Figures 2a–h) are generated by filtering the data so that if the two consecutive configurations share the same value a small line is drawn, but if the values are not identical, the pen is moved without drawing a line.

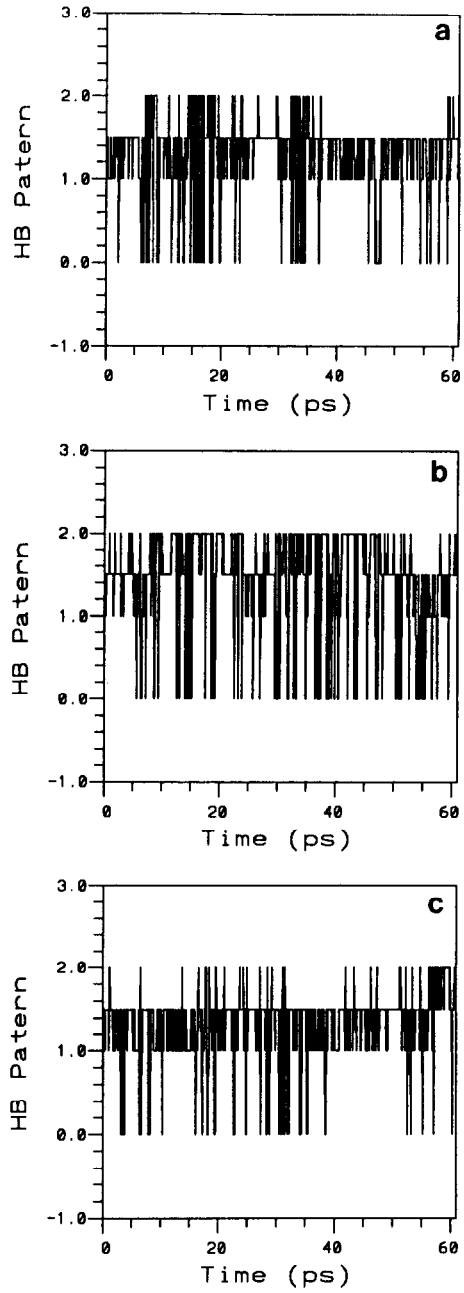

Figure 1. Trajectory for the three-center hydrogen bonding states with the values 0, 1, 1.5, and 2 for the states corresponding to no hydrogen bond, normal Watson–Crick hydrogen bond, three-center hydrogen bond, and secondary hydrogen bond, respectively: a, three-center hydrogen bonding formed by N1–H of the residue G2 with N3 and O2 of residue C11; b, three-center hydrogen bonding formed by N1–H of the residue G3 with N3 and O2 of residue C10; and c, three-center hydrogen bonding formed by N1–H of the residue G5 with N3 and O2 of residue C8.

RESULTS AND DISCUSSION

Schematic representation of hydrogen bonding

Schematic representation of the hydrogen bonding between the $d(G)_6$ and $d(C)_6$ strands for different MD time slices is shown in Color Plate 1. The arrows point from donor to acceptor with a thickness proportional to the frequency of occurrence obtained from the MD simulation. Only donor and acceptor atoms are shown in this diagram. The horizontal arrows represent normal Watson–Crick-type hydrogen bonds. It can be seen that throughout the simulation, regardless of the base pair examined, the major groove O6(G) · · H–N4(C) hydrogen bonds occur less frequently than the minor groove N2(G)–H · · O2(C) hydrogen bonds.

Figure 2. Trajectory of the states of the three-center hydrogen bonding were performed by assigning the values 0, 1, 1.5, and 2 for the states corresponding to no hydrogen bond, normal Watson–Crick hydrogen bond, three-center hydrogen bond, and secondary hydrogen bond, respectively. A filter is applied to plot only the state which persists for more than two consecutive configurations: a, three-center hydrogen bonding formed by N1–H of residue G2 with N3 and O2 of residue C11; b, three-center hydrogen bonding formed by N1–H of residue G3 with N3 and O2 of residue C10; c, three-center hydrogen bonding formed by N1–H of residue G5 with N3 and O2 of residue C8; d, three-center hydrogen bonding formed by N4–H of residue C11 with O6s of residues G1 and G2; e, three-center hydrogen bonding formed by N4–H of residue C10 with O6s of residues G2 and G3; f, three-center hydrogen bonding formed by N4–H of residue C9 with O6s of residues G3 and G4; g, three-center hydrogen bonding formed by N4–H of residue C7 with O6s of residues G5 and G6; and h, three-center hydrogen bonding formed by N2–H of residue G3 with O2s of residues C10 and C11.

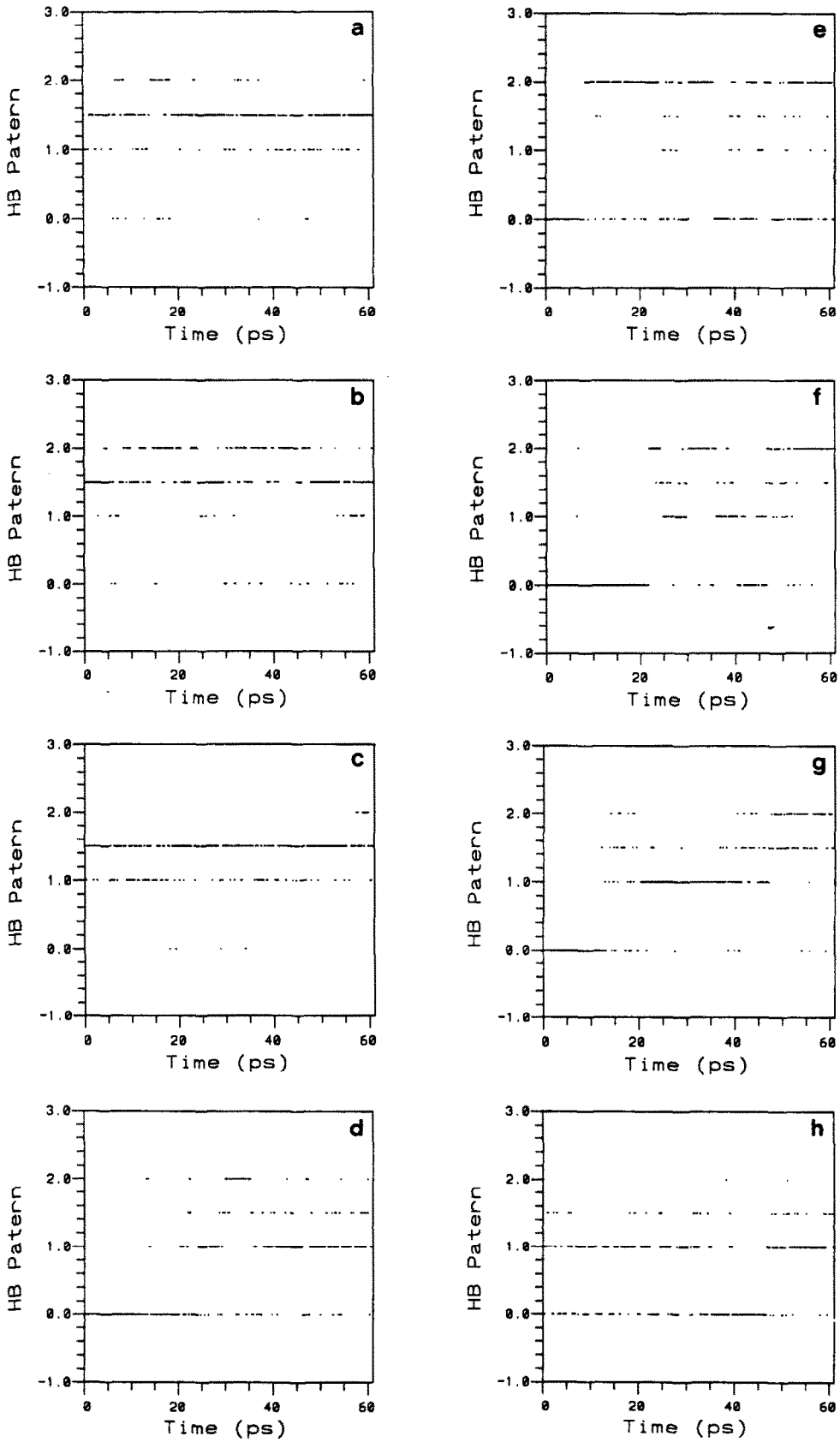
a
b
c
d
e
f
g
h
HB Patern
Time (ps)
3.0
2.0
1.0
0.0
-1.0
0
20
40
60

The arrows are also color coded to assist in the recognition of different types of hydrogen bonds. Black is used for a normal Watson–Crick hydrogen bond, while blue is used to represent the additional N1(G)–H··O2(C) hydrogen bond that is formed for most of the G·C base pairs within their own base-pair planes. The thickness indicates that some of these non-Watson–Crick-type hydrogen bonds occur as frequently as the standard Watson–Crick bonds. Also, there are several hydrogen bonds that are formed between two adjacent base pairs. Two types dominate this class of unusual hydrogen bonds. In one type, the N4 of cytosine interacts with an O6 of an adjacent guanine in the major groove while maintaining a normal Watson–Crick hydrogen bond with the O6 of its own guanine in the base-pair plane. These bonds are shown as arrows pointing to the upper left in red. The diagram clearly indicates that this is a rather common occurrence throughout the simulation, but the frequencies fluctuate from one time span to another as well as from one base pair to another. It should be pointed out that this type of unusual hydrogen bonding has been observed in the crystal structures of deoxyoligonucleotide duplexes.[23,24] A less dominant minor groove counterpart is shown as arrows pointing to the upper right, also in red. Here the N2 of a guanine interacts with the O2 of two cytosines, one within its own base-pair plane and the other in the base-pair plane adjacent to it. The thinness of these arrows indicates that this type of unusual hydrogen bonding occurs much less frequently than the major groove counterpart. Since the hydrogen atoms in these three types of unusual hydrogen bonding are also involved in normal Watson–Crick hydrogen bonding, they contribute to three-center hydrogen bonding, which will be discussed later in more detail. Both hydrogen atoms of the guanine N2 (H and H′) are capable of forming a hydrogen bond with the O2 of an adjacent cytosine. However, since the second hydrogen (H′) is not involved in the normal Watson–Crick hydrogen bond formed within the base pair, it is not involved in the formation of a three-center hydrogen bond. This type of hydrogen bond N2(G)–H′··O2(C) occurs less frequently than the N2(G)–H··O2(C) bonds discussed above and is shown in green, as are other minor bonds.

Hydrogen bonding distance and angle trajectory plots

Although changes in the frequencies of individual bonds can be seen from changes in thickness of arrows in the schematic presentation, trajectory plots more clearly represent the dynamic nature of hydrogen bonding, e.g., the stable normal Watson–Crick hydrogen bond in Color Plate 2a for N2(G1)–H··O2(C12). Both the H(N2)··O2 distance (blue) and the N2–H··O2 angle (red) remain within the upper and lower horizontal limits. This turns out to be one of the exceptional cases. More typical behavior is shown by the N1(G3)–H··N3(C10) Watson–Crick bond (Color Plate 2b), for which the angle (red) remains in an acceptable region most of the time but the distance (blue) tends to be too long. This Color Plate also shows a hydrogen bond fluctuating between formation and breakage during the simulation period.

The non-Watson–Crick hydrogen bonds, N1(G)–H··O2(C), shown in blue arrows in Color Plate 1 do not often satisfy the normal linear hydrogen bonding criteria (0.25 nm for H··A distance and 135° for D–H··A angle) as shown in Color Plate 2c for the N1(G5)–H··O2(C8) bond. If the more relaxed criteria (0.27 nm for the H··A distance and 90° for the D–H··A angle) are used, the majority of N1(G)–H··O2(C) bonds satisfy this condition most of the time even from the beginning of the simulation, as shown for the N1(G5)–H··O2(C8) bond in Color Plate 2d. All six bonds of this type (others not shown) display a similar pattern.

The dynamic details of unusual hydrogen bonding between adjacent base pairs (red and green arrows in Color Plate 1) are also interesting. The Color Plates 2e and 2f present examples of unusual hydrogen bonds formed between adjacent base pairs in the major groove. The N4(C9)–H··O6(G3) bond (Color Plate 2e) forms rather late (21 ps) in the simulation. After formation, the angular criterion is satisfied most of the time so that the presence of hydrogen bonding depends on the distance criterion alone. Similar features are observed in the trajectories for all four other bonds of this type (the N4(C7)–H··O6(G5) bond is shown in Color Plate 2f). The changes in thickness of the arrows shown in Color Plate 1 are clearly reflected in this diagram. The situation for the minor groove counterpart, N2(G)–H··O2(C), is slightly different, as shown for the N2(G4)–H··O2(C10) bond in Color Plate 2g. Here the hydrogen bonding criteria are satisfied early in the simulation but both the distance and the angle frequently go beyond the cutoff during the simulation. Similar patterns are observed for the other minor groove hydrogen bonds not involved in Watson–Crick hydrogen bonding. An example of this type of bond, the green arrows in Color Plate 1, is shown for N2(G6)–H··O2(C8) in Color Plate 2h, similar to Color Plate 2g. In the major groove counterpart, N4(C9)–H··O6(G3) (Color Plate 2i), the hydrogen is not involved in Watson–Crick hydrogen bonding. By comparing Color Plate 2i to Color Plate 2e it can be seen that the O6(G3) interacted with one of the N4(C9) amino hydrogens at the beginning of the simulation but then later switched to interact with the other N4(C9) amino hydrogen. This may have been achieved by the rotation of the exocyclic amino group.

Three-center hydrogen bonds

Systematic analysis of three-center hydrogen bonding was done using crystal structures obtained from the neutron diffraction studies[25] of pyranoses and pyranosides,[26] small organic compounds,[27] amino acids,[28] nucleosides and nucleotides,[29] and barbiturates, purines and pyrimidines.[30] In organic crystals, it is commonly observed that one component of a three-center hydrogen bond is shorter in length and closer to linear than the other. This indicates that the two components are not equal in strength. The schematic presentation of the hydrogen bonding in the $d(G)_6 \cdot d(C)_6$ MD simulation (Color Plate 1) also shows that at times one hydrogen atom is shared by two different acceptor atoms. The possible three-center hydrogen bonds are grouped into the following three different types, where the symbol *n* indicates the *n*th base pair.

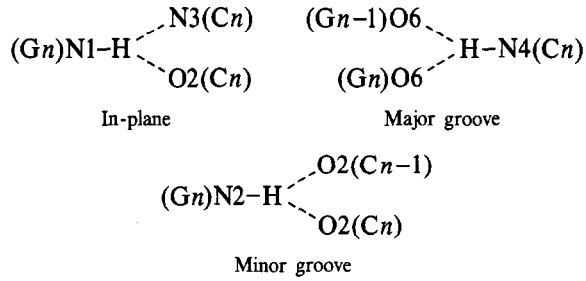

Trajectory plots of parameters defining the three-center hydrogen bonds were created for the above three different types to examine their dynamic behavior. Some of these are shown in Color Plates 3a–i. The first example is for an in-plane three-center bond formed by N1–H of residue G2 with N3 and O2 of residue C11. In Color Plates 3a and 3b the normal Watson–Crick hydrogen bond is drawn in blue and the N1(G2)–H · · O2(C11) bond is drawn in red with hydrogen bonding cutoffs given as black horizontal lines. The H · · A distance (Color Plate 3a) shows a fluctuation in the relative strength of hydrogen bonding, as judged by the shortness of these bonds. Sometimes the H · · A distance is shorter for the normal Watson–Crick hydrogen bond (blue), and sometimes this distance is shorter for non-Watson–Crick hydrogen bond (red). However this fluctuation in dominance is not carried over to the angle test (Color Plate 3b) where the normal Watson–Crick hydrogen bonding (blue) falls consistently closer to linear than the non-Watson–Crick hydrogen bonding (red). This indicates that for some cases, either the angle parameter is not a sensitive measure of the dominant components, or the distance parameter does not reflect the strength of the dominant component. Color Plate 3c shows the trajectory for the sum of three angles around the hydrogen (orange) and the dihedral angle A1–D–H–A2 (purple). Although both of these parameters describe the degree of coplanarity of the three-center hydrogen bonding atoms, their sensitivities are totally different. The dihedral angle remained within the hydrogen bonding limits while the sum of three angles shows large fluctuations and tends to deviate frequently from the hydrogen bonding condition. Color Plates 3d–f are the trajectories for the in-plane three-center bond formed by N1–H of residue G3 with N3 and O2 of residue C10. Again the sum of three angles is much more sensitive than the dihedral angle (Color Plate 3f). For this base pair, the distance diagram (Color Plate 3d) clearly indicates that the N1–H · · O2 bond is stronger than the Watson–Crick N1–H · · N3 bond. However, the dominant form is not clear from the angle diagram (Color Plate 3e). Although the sum-of-three-angles parameter is a more sensitive planarity measure than the dihedral angle parameter, it is still difficult to determine the dominant component of in-plane three-center hydrogen bonding by using the distance and angle parameters. This may be due to the fact that for in-plane three-center hydrogen bonding, the two components are both strong hydrogen bonds.

The N4(C9)–H hydrogen bonding with the O6s of G3 and G4 (Color Plates 3g–i) typifies a major groove three-center hydrogen bond. For this group of atoms, no hydrogen bonding is detected near the beginning of the simulation using the H · · A distance, D–H · · A angle and the sum-of-three-angles criteria. Relatively large negative values of the dihedral angle are within the specified cutoff and indicate weak hydrogen bonding. Only at 22 ps do all the parameters simultaneously start to show the existence of three-center bonding. It is clear both from the distance and angle diagrams that the normal Watson–Crick hydrogen bond and the cross strand adjacent-pair hydrogen bond take turns dominating. Although the details differ for each residue, these overall trends are similar for all the major groove three-center hydrogen bonds examined.

The minor groove three-center bond is shown for the bond formed by the N2(G3)–H and the O2s of residues C10 and C11 (Color Plates 3j–l). In contrast to the two previously examined three-center bonds, this one shows clear dominance of the normal Watson–Crick hydrogen bond. Although the angle D–H · · A2 (Color Plate 3k) and the dihedral angle (Color Plate 3l) parameters for the cross strand adjacent-pair hydrogen bond meet the criteria for hydrogen bonding most of the time, the distance H · · A2 (Color Plate 3j) and the sum of three angles (Color Plate 3l) show that they exceed the criteria very often either because the secondary hydrogen bond between adjacent base pair tends to be too long or the D–H · · A2 angle tends to be too small.

Three-center hydrogen bond and flip-flop hydrogen bond

It is important to distinguish between stable three-center hydrogen bonding and the flip-flop hydrogen bonding that may occur when two hydrogen bond acceptors share a common hydrogen. For the former, the hydrogen bonding condition, including the planarity condition for the atoms involved, must be satisfied simultaneously for both bonds. In the latter case, one bond satisfies the hydrogen bonding condition while the other cannot; i.e., one bond starts to break when the other starts to form, repeatedly switching back and forth so that only one hydrogen bond exists at any given time. It has been suggested from the MD study of carbohydrates[9,10] that three-center hydrogen bonding serves as an intermediate state for flip-flop hydrogen bonding. While the Color Plates 3a–l provide some clues to the dynamic nature of three-center hydrogen bonding, a better pictorial analysis tool was needed to discover whether it serves as an unstable intermediate state for flip-flop hydrogen bonding.

As described above, the values 0, 1, 1.5, and 2 were assigned to the states corresponding to no hydrogen bond, a normal Watson–Crick hydrogen bond, a three-center hydrogen bond, and a secondary hydrogen bond formed in a base-pair plane, major groove or minor groove, respectively. For states 1 and 2, the normal linear hydrogen bonding criteria were applied, while for the state 1.5 the three-center hydrogen bonding criteria were used.

These values are plotted as a function of time in Figures 1a–c for the in-plane three-center hydrogen bonds formed between N1–H of guanine and N3 and O2 of cytosine of the G2–C11, G3–C10 and G5–C8 pairs, respectively. The three-center hydrogen bonds (1.5) are stable for the entire simulation period with many short interruptions caused by the formation of a normal Watson–Crick N1(G)–H · · N3(C) bond (Figure 1c), an unusual N1(G)–H · · O2(C) hydrogen bond (Figure 1b), or both (Figure 1a). The interruption due to the no-hydrogen-bond state was not common. Interpre-

tation is facilitated by using a filter to plot only two or more consecutive occurrences of the same state (Figures 2a–c). The filter eliminates transient (0.05 ps) changes between states. Again, it is shown that the in-plane three-center hydrogen bonds are very stable.

A different situation exists for the major and minor groove adjacent base-pair three-center hydrogen bonds. The image for the major groove three-center hydrogen bonds formed between the N4–H (Cn) and O6s (Gn–1, Gn) appears in Figures 2d–g for hydrogen bonding involving C11–G1 and G2, C10–G2 and G3, C9–G3 and G4, and G7–G5 and G6 pairs, respectively. The minor groove counterpart involving N2(Gn)–H and O2s (Cn, Cn–1) is shown in Figure 2h for the G3–C10, C11 pairs. Each diagram shows that the three-center bonds formed by adjacent base pairs along the grooves are not stable. In Figures 2d–h the secondary hydrogen bonding in the minor groove, N2(Gn)–H · · O2(Cn–1), rarely forms a normal linear hydrogen bond, while the major groove counterpart, N4(Cn)–H · · O6(Gn–1) frequently forms a normal hydrogen bond. The behavior of major groove three-center hydrogen bonding depends strongly on the individual hydrogen bonds making up the pairs. In Figure 2d there is an initial no-hydrogen-bond period after which a normal Watson–Crick hydrogen bond is formed and then interrupted by the secondary hydrogen bond for a short period. The three-center bond appears as a transient state. Figure 2e shows the case where the secondary hydrogen bond dominates over the Watson–Crick type bond. In this diagram the three-center bond appears to be an intermediate step connecting the state having no hydrogen bond with one having a strong secondary normal linear hydrogen bonding. Figure 2f presents the case where the Watson–Crick hydrogen bond and the secondary hydrogen bond frequently alternate in dominance. Here the three-center bond seems to act as an intermediate state between the switches in dominant hydrogen bonding forms. This may be considered as the typical flip-flop hydrogen bonding pattern. The last example of major groove hydrogen bonding appears in Figure 2g. In this figure an initial no-hydrogen-bond state is followed by a period dominated by Watson–Crick type hydrogen bonding. This is followed by a period in which a secondary hydrogen bonding state alternates with a three-center hydrogen bonding state until the end of the simulation. The minor groove example (Figure 2h) shows that during the entire simulation period the Watson–Crick hydrogen bonding and no-hydrogen-bond state alternate in dominance. Here the three-center hydrogen bonding state may be serving as the intermediate state between these two states. This is similar to the example shown in Figure 2e, except that the secondary hydrogen bonding takes the place of the Watson–Crick bond.

CONCLUSION

This study demonstrates that the schematic drawing of hydrogen bonding patterns between base pairs and various trajectory plots are essential tools in analyzing the nature of hydrogen bonding during an MD simulation.

In nucleic acid fragments three-center hydrogen bonds can be classified into three different types: in-plane, major groove, and minor groove. Among these three-center hydrogen bonding types, the in-plane three-center bond is the most stable and the minor groove three-center bond is the least stable. The in-plane three-center hydrogen bonds tend to dominate over the individual linear hydrogen bonding components. They represent a stable three-center hydrogen bonding state in which both bonds simultaneously satisfy relaxed hydrogen bonding criteria over a long period. On the other hand, the groove three-center hydrogen bonds behave as transient intermediates connecting two different states. They may be connecting the no-hydrogen-bond state with other states, or they may be linking two different linear hydrogen bonding states. In the latter case, they act as an intermediate state for a flip-flop hydrogen bonding system.

REFERENCES

1 Pimentel, G.C. and McClellan, A.L. *The Hydrogen Bond.* W.H. Freeman, San Francisco (1960)
2 Hamilton, W.C. and Ibers, J.A. *Hydrogen Bonding in Solids.* W.A. Benjamin, New York (1968)
3 Vinogradov, S.N. and Linnell, R.H. *Hydrogen Bonding.* van Nostrand Reinhold, New York (1971)
4 Toniolo, C. *CRC Crit. Rev. Biochem.* 1980, **9**, 1–44
5 Baker, E.N. and Hubbard, R.E. *Prog. Biophys. Mol. Biol.* 1984, **44**, 97–179
6 Saenger, W. *Ann. Rev. Biophys. Biophys. Chem.* 1987, **16**, 93–114
7 Westhof, E. *Ann. Rev. Biophys. Biophys. Chem.* 1988, **17**, 125–144
8 Legon, A.C. *Chem. Soc. Rev.* 1990, **19**, 197–237
9 Koehler, J.E.H., Saenger, W. and van Gunsteren, W.F. *J. Biomol. Struct. Dyn.* 1988, **6**, 181–198
10 Koehler, J.E.H., Saenger, W. and van Gunsteren, W.F. *Eur. Biophys. J.* 1988, **16**, 153–168
11 Swanson, S.M., Wesolowski, T., Geller, M. and Meyer, E.F. *J. Mol. Graphics* 1989, **7**, 240–242
12 Nordlund, T.M., Anderson, S., Nilsson, L., Rigler, R., Gräslund, A. and McLaughlin, L.W. *Biochemistry* 1989, **28**, 9095–9103
13 Fraternali, F. *Biopolymers* 1990, **30**, 1083–1099
14 McCammon, J.A. and Harvey, S.C. *Dynamics of Proteins and Nucleic Acids.* Cambridge University Press, Cambridge (1987)
15 Levitt, M. *Cold Spring Harbor Symp. Quant. Biol.* 1983, **47**, 251–275
16 Singh, U.C., Weiner, S.J. and Kollman, P.A. *Proc. Natl. Acad. Sci. U.S.A.* 1985, **82**, 755–759
17 van Gunsteren, W.F., Berendsen, H.J.C., Geurtsen, R.G., and Zwinderman, H.R.J. *Annals N.Y. Acad. Sci.* 1986, **482**, 287–303
18 Zielinski, T.J. and Shibata, M. *Biopolymers* 1990, **29**, 1027–1044
19 Arnott, S., Smith, P.J., and Chandrasekaran, R. *CRC Handbook of Biochemistry and Molecular Biology: Nucleic Acids. Third edition* (G.D. Fasman, Ed.) CRC Press, Cleveland (1976) Vol. 2, pp. 411–422
20 Berendsen, H.J.C., Postma, J.P.M., van Gunsteren, W.F. and Hermans, J. *Intermolecular Forces* (B. Pullman, Ed.) D. Reidel, Dordecht (1981) pp. 331–342
21 van Gunsteren, W.F. and Berendsen, H.J.C. *Groningen*

Molecular Simulation System, BIOMOS b.v. Biomolecular Software, Laboratory of Physical Chemistry, University of Groningen, Groningen, The Netherlands (1986)
22 Murray-Rust, P. and Glusker, P. *J. Am. Chem. Soc.* 1984, **106**, 1018–1025
23 Heinemann, V. and Alings, C. *J. Mol. Biol.* 1989, **210**, 369–381
24 Timsit, Y., Westhof, E., Fuchs, R.P.P. and Moras, D. *Nature* 1989, **341**, 459–462
25 Ceccarelli, C., Jeffrey, G.A., and Taylor, R. *J. Mol. Struct.* 1981, **70**, 255–271
26 Jeffrey, G.A. and Mitra, J. *Acta Crystallogr.* 1983, **B39**, 469–480
27 Taylor, R., Kennard, O., and Versichel, W. *J. Am. Chem. Soc.* 1984, **106**, 244–248
28 Jeffrey, G.A. and Mitra J. *J. Am. Chem. Soc.* 1984, **106**, 5546–5553
29 Jeffrey, G.A., Maluszynska, H., and Mitra, J. *Int. J. Biol. Macromol.* 1985, **7**, 336–348
30 Jeffrey, G.A. and Maluszynska, H. *J. Mol. Struct.* 1986, **147**, 127–142